Activation parameters of conjugated polyaniline electrolyte via dielectric relaxation technique

Ifeanyichukwu C Amaechi[a,b]*, Bashiru B Balogun[b,c], Michael I Nwachukwu[b], Celia T Sousa[c], Gleb N Kakazei[c],
João P Araújo[c] & Rose U Osuji[b,d,e]

[a]Institut National de laRecherche Scientifique, Centre Énergie, Matériaux & Télécommunications (INRS-EMT),
Universitè du Quèbec 1650, Boulevard Lionel-Boulet Varennes J3X 1S2, Quèbec, Canada

[b]Department of Physics and Astronomy, University of Nigeria Nsukka, Enugu State, Nigeria

[c]IFIMUP and IN Institute of Nanoscience and Nanotechnology/Department of Physics and Astronomy, University of Porto,
Rua do Campo Alegre 687, 4169-007 Porto, Portugal

[d]Nanosciences African Network (NANOAFNET), iThemba LABS-National Research Foundation, 1 Old Faure road,
Somerset West 7129, POBox 722, Somerset West, Western Cape Province, South Africa

[e]UNESCO-UNISA Africa Chair in Nanosciences/Nanotechnology, College of Graduate Studies, University of South Africa (UNISA),
Muckleneuk ridge, PO Box 392, Pretoria South Africa

The synthesis and relaxation mechanism of polyaniline electrolyte in form of thin film by oxidative polymerization in the presence of inorganic acid have been reported. The films have been characterized by scanning electron microscopy (SEM), Fourier transform infrared (FTIR) spectroscopy, 2-point probe and UV-Vis absorption spectroscopy. The mechanism of electrical conductivity for the disordered system has been explained in terms of Mott's variable-range hopping for the intrinsic conduction of the protonated long chain. The dielectric parameters including real part, imaginary part and loss tangent have been measured between the wavelength range 400 – 1100 nm. These have been employed in the determination of dielectric relaxation time τ which exhibits Arrhenius-like behaviour. Finally, the temperature dependent relaxation time which is a function of activation energy of dipole orientation otherwise known as Gibbs free energy $\Delta G^{\#}$, has been utilized in estimation of some thermodynamic parameters such as enthalpy $\Delta H^{\#}$ and entropy $\Delta S^{\#}$. The SEM shows an aggregation of randomly oriented fibrous network of polyaniline on the surface of substrate. Fourier transform infrared confirms the acoustic vibrational modes of the long chain polymer.

Keywords: Dielectric relaxation, Enthalpy, Electrical conductivity, Gibbs free energy

1 Introduction

Electrically conducting polymers described as a new class of synthetic metals reached a high interest in the last years, confirmed by the 2000 Nobel Prize in chemistry for the discovery and development of conductive polymers[1]. After the theoretical prediction of room temperature ferromagnetism in wide band gap based semiconductors, conjugated polymers (CPs) including polythiophene[2,3] polypyrrole (PPy)[4,5], poly(DNTD)[6-8], polyaniline (PANi)[9,10] and their derivatives have attracted huge attention. Polyaniline conventionally procured by mineralization of acid into –N= sites is one of the most studied materials because of its intriguing properties such as high conductivity upon doping with acids, well-behaved electrochemistry, and easy preparation under reproducible conditions by electropolymerization and chemical oxidation of aniline, electrochemical and good environmental stability[11-19], facile polymerization in aqueous media[20-23] or non-aqueous media[24], versatile redox behavior, low cost, high conductivity, and high pseudocapacitance[25,26].

Since they belong to long-chained (conjugated) organic materials, the molecular dynamics of this protonated polymer in non-polar solvents is yet to be understood. To unravel the mystery surrounding the rotational motion of a dipolar unit of a polar polymer in dilute solution, dielectric relaxation technique has been employed. Dielectric techniques have proved particularly effective in the study of polymer dynamics at interfaces and in confining geometries of polymers in ultrathin films or within nanometric pores of oxide glasses, polymer in the galleries of clays, etc.[27] because of their enhanced sensitivity with decreasing size scale in an unparalleled range of

---

*Corresponding author
(E-mail: ifeanyichukwu.amaechi@emt.inrs.ca)

frequency and temperature[28,29]. This conventional technique has a particular advantage of monitoring the cooperative motion of molecular ensemble which distinguishes it from Raman spectroscopy that yields information on the motions of individual molecules[30]. In other words, it is a valuable tool for investigation of liquids whose structure and dynamics are dominated by intermolecular hydrogen bonds[31]. Data on relaxation behaviour procured from dielectric measurements have become the basis for the study of thermodynamic parameters[33-37] such as change in activation energy ΔG_τ^*, enthalpy of activation ΔH_τ^*, entropy of activation ΔS_τ^*. The Whiffen and Thompson model[32] as employed by Hosamani *et al.*[33] and Sannaningannavar et al.[38] has become one of the most effective ways of determining the probable relaxation time τ, real part ε' and imaginary component ε'' of a complex dielectric permittivity $\varepsilon^* = \varepsilon' \pm j\varepsilon''$. Even though the model has been modified to accommodate and deal with the likely existence of more than one single frequency, culminating into appropriate values of thermodynamic parameters, dipole moments etc as predicted by Higasi[39] and Higasi *et al.*[40], this does not invalidate the fact that the aforesaid model provided useful and precise thermodynamic information.

For example, Hosamani *et al.*[33] studied the activation energy (ΔG^*), enthalpy (ΔH^*), and entropy (ΔS^*) of some indoles and certain of their binary mixtures. Also, the dielectric relaxation of water between 0 °C and 35 °C was investigated by Buchner *et al.*[41] Here, the description of the complex dielectric spectra and data require a superposition of two Debye processes which was matched with literature results to cover frequency range $0.2 \leq \upsilon /\text{Ghz} \leq 410$. Again, the aforesaid model was extended to polyethylene glycol (PEG) where its chemical behaviour in non-polar solvent was measured and established[38].

Since the optical and electrical properties of polyaniline is known to vary with its different oxidation states and forms, several deposition techniques have been employed to fabricate this polymer with optimized properties. According to literature, some of the methods include electrochemical[42], seeding[43], sonochemical polymerization, plasma, chemical solution etc. Chemical solution involving oxidative polymerization of aniline is advantageous due to layer-by-layer growth and comprises excellent material utilization efficiency, good control over deposition process along with film thickness and specifically convenient for large area deposition on virtually any type of substrate.

Although great deal of work based on dielectric relaxation for the determination of some physical thermodynamic observables of conjugated polymers employing Whiffen and Thompson model had been reported, none had been linked to polyaniline to the best of our knowledge. In the light of this, the present study discusses the kinetics and determination of activation parameters of polyaniline formation using dielectric relaxation technique. Results obtained are used to explain the resonance of the electronic polarization of the long-chain polymer.

2 Methods and Experimental Details

Analytical grades of aniline (C_6H_7N), 35% hydrochloric acid (HCl), and ammonium persulfate (APS, $(NH_4)_2S_2O_8$) from Sigma-Aldrich were used as received without further purification. The chemical route for realization of polyaniline involves an oxidative polymerization of anilinium ion in inorganic acid by APS. The chemical bath deposition (CBD) and stoichiometric conditions were described elsewhere[45]. Briefly, the bath consisted of solutions of 2 mL aniline, 1 M 30 mL HCl, and 0.25M 20 mL APS dissolved in 1 M HCl. Quartz substrates were immersed vertically in the mixture at ambient temperature. After 2 h, polyaniline films were removed and rinsed with distilled water. Preparation of thicker films may be carried out by re-inserting the initially deposited films into a fresh bath. The morphology and molecular bonding of polyaniline were characterized with a scanning electron microscopy, SEM (LEO (Zeiss) 1540) and Fourier transform infrared spectrometer, FTIR (Thermo Nicolet NEXUS 870) respectively. To determine the temperature dependence of relaxation time $\tau(T) = \tau_o \exp\left(\dfrac{\Delta G^{\#}}{k_B T}\right)$, an expression (see Eq. (1)) for dielectric loss, tan δ, comprising both real and imaginary part of dielectric constant was used. Therefore, the dielectric constants were determined via the transmission and reflection spectra obtained from CARY 5E UV-Visible spectrophotometer. Electrical resistivity was measured as a function of temperature by forming metal-sample-metal structure of dimension 1 cm x 1 cm with silver (Ag) paste contact by 2-point probe method [45] using a source meter. The resistivity was studied in the temperature range 300 – 330 K.

$$\tan \delta = \left[\frac{\left(\varepsilon'+1\right)^2}{\varepsilon'}\right]\left[\frac{\left(4\pi CN\mu^2\right)}{27Vk_BT}\right]\left[\frac{\omega\tau}{\left(1+\omega^2\tau^2\right)}\right] = \frac{\varepsilon''}{\varepsilon'}$$

$$\cdots (1)$$

Where ε' and ε'' are the real imaginary part of dielectric constant, respectively, ω the angular frequency and μ is the dipole moment of polar solid film. The relaxation time is connected to activation energy $\Delta G^{\#}$ according to transition state theory of Eyring equation:

$$\tau = \left(\frac{h}{k_BT}\right)\exp\left(\frac{\Delta G^{\#}}{RT}\right) \qquad \cdots (2)$$

and $\Delta G^{\#} = -2.303RT\,Log\left(\dfrac{\tau k_BT}{h}\right)$ conforms with the

obtention of activation energy. The system under consideration is however at constant temperature and pressure, chemical reaction is spontaneous in the direction of decreasing Gibbs energy as given by Eq. (3):

$$\Delta G^{\#} = \Delta H^{\#} - T\Delta S^{\#} \qquad \cdots (3)$$

where k_B is the Boltzmann constant, R is gas constant, h is Planck's constant, $\Delta H^{\#}$ and $\Delta S^{\#}$ are change in enthalpy and entropy, respectively.

Equation (2) can be rewritten to accommodate relaxation time which takes the form:

$$Log\left(\frac{\tau k_BT}{h}\right) = -\frac{\Delta H^{\#}}{2.303R}\left[\frac{1}{T}\right] + \frac{\Delta S^{\#}}{2.303R} \qquad \cdots (4)$$

Therefore, the linear graph of $Log\left(\dfrac{\tau k_BT}{h}\right)$ against

inverse of temperature (T^{-1}) produces a slope $-\dfrac{\left(\Delta H^{\#}\right)}{2.303R}$ from which the change in enthalpy $\Delta H^{\#}$ can be determined and the intercept yields change in entropy which can as well follow from Eq. (2).

3 Results and Discussion

To comprehend the electron transport behaviour within the conducting polymer, the electronic transport mechanism can be clarified by investigating the temperature dependent conductivity as given by Eq. (5):

$$\sigma = \sigma_o \exp\left(-\left(T_0/T\right)^{1/4}\right) \qquad \cdots (5)$$

where all the symbols retain their usual meaning[44]. Figure 1 shows the variation of conductivity with temperature. The activation energy of an intrinsic conduction was found to be 1.36×10^{-20} J and this is shown by the linearity that exist between ln $(\sigma T^{1/2})$ and $T^{1/4}$ within the aforesaid temperature range. Both the conductivity and activation energy are in agreement with the reports of Singh et al.[46]. Hence, this mechanism of conduction strongly supports the proposition of Wang et al.[47] that HCl-doped emeraldine salt consists of coupled parallel chains that form ''metallic'' bundles. This effect seemed to culminate from the π-π stacking or chain containing bond sequence, an important factor that facilitates the electron transport within the matrix.

The isothermal variation of real component ε_r of the dielectric constant with wavelength is presented in Fig. 2. Viewed from a microscopic perspective, it is known that the molecular polarizability is frequency
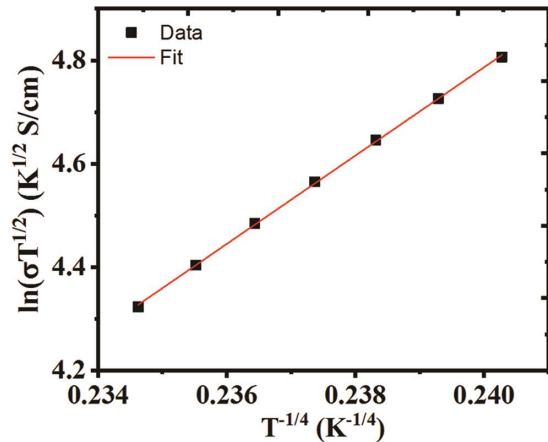

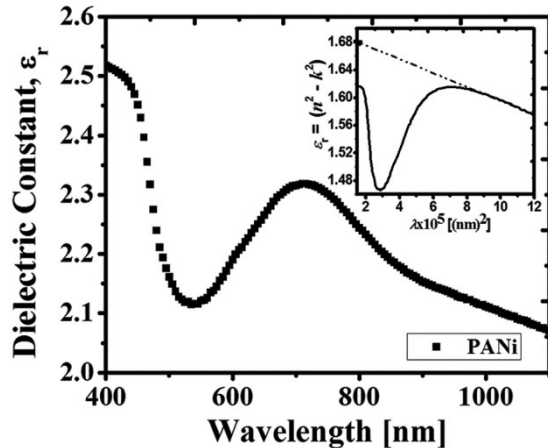Fig. 1 — ln$(\sigma T^{1/2})$ versus $T^{1/4}$ curve for polyaniline film.

Fig. 2 — Ambient temperature variation of dielectric permittivity (real) with wavelength. Inset shows the plot of dielectric permittivity $\varepsilon_r = n^2 - k^2$ versus square of wavelength, λ^2.

dependent. The high frequency response can follow the undulations of electromagnetic radiation in the visible region and hence this response gives rise to refraction of light. This contribution is the high frequency or optical dielectric constant ε_∞. Since the phenomenon is entirely electronic transition caused by high frequencies, we are not much interested in changes in the electrical response due to dipolar reorientation, that is, static dielectric constant. Hence, the real component of the dielectic constant shows a dependence on the square of wavelength according to Spitzer and Fan[48]. The plot of $\varepsilon_r = n^2 - k^2$ vs. λ^2 (see inset of Fig. 2) with intercept on ε_r axis (i.e., $\lambda^2 = 0$) for the linear part at shorter wavelengths gives the high frequency dielectric constant 1.68.

Inset of Fig. 3 shows the loss tangent plot obtained via Eq. (1) as a function of square of wavelength. The curve shows a sharp increase between 400 - 450 nm and later decreased as it approached 500 nm. Obviously, it was evident that spontaneous rise in dielectric loss from visible to the near infrared (NIR) which almost remained stable in the high frequency zone was due to induction of polarization at high frequencies. Similar observation was recorded by Zhu *et al.*[49] for pure polyaniline and nanostructure-derived polyaniline metacomposites. To deduce the enthalpy, the variation of $\ln(\tau k_B T/h)$ against T^{-1} was plotted as shown in Fig. 3. The low wavelength dielectric constants procured at ambient temperature alongside temperature dependent relaxation time and thermodynamic parameters $\Delta G^\#$, $\Delta H^\#$ and $\Delta S^\#$ for the protonated polymer are presented in Table 1. Relaxation time constitutes an important parameter in dielectric studies as it is connected with transition probabilities between consecutive minimum energy configurations of the dipoles[50].

Figure 4 shows the temperature dependence of the relaxation time. The almost linearity of the plot establishes the fact that it follows a Debye process and not the relaxation mechanism of dipoles originating from complex forms of molecular or ionic

motion as described by the semi-empirical Williams-Landel-Ferry (WLF) equation[51]. Hence, there is a possibility of existence of more than one relaxation process in the molecule. At elevated temperature, the measured relaxation times are in good agreement with those of Sannaningannavar *et al.*[38] for PEG obtained using modified Whiffen and Thompson model[52]. However, there is a decreasing trend associated with
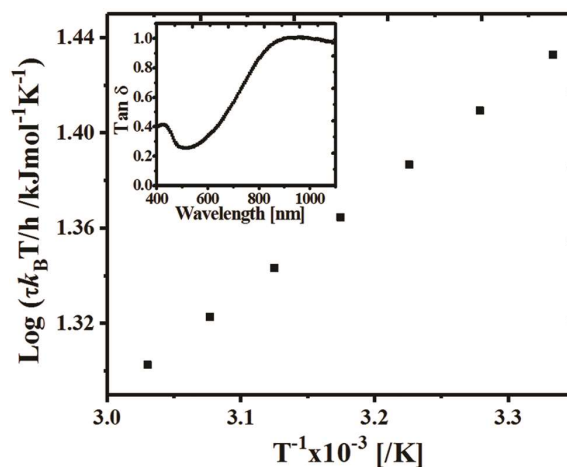

Fig. 3 — Plot for determination of enthalpy $\Delta H^\#$ of polyaniline. Inset shows ambient temperature variation of loss tangent (tan δ) with wavelength.
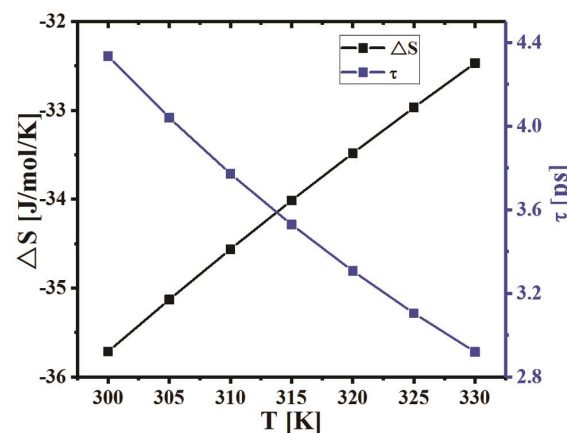

Fig. 4 — Temperature dependence of entropy $\Delta S^\#$ and relaxation time.

Table 1 — Estimated values of dielectric permittivity (real), thermodynamic parameters and relaxation time at different temperatures

Polymer	ε' @400 nm	ε_∞	$\Delta G^\#$ (J/mole)	$\Delta H^\#$ (J/mole)	$\Delta S^\#$ (J/mole/K)	τ (ps)	T (K)
Polyaniline	2.52	1.68	-8230.48(3372)	-18944.76	-35.7143	4.34	300
			-8230.48(2362)		-35.1288	4.04	305
			-8230.48(2771)		-34.5622	3.77	310
			-8230.48(3167)		-34.0136	3.53	315
			-8230.48(2207)		-33.4821	3.31	320
			-8230.48(2600)		-32.9670	3.11	325
			-8230.48(2981)		-32.4675	2.92	330

the values of τ as temperature increases. The explanation is thus since polyaniline was formed in a non-isomeric medium in the presence of dilute inorganic acid, this notable trend clearly does depend on the location of dipole in the polymer matrix, nature and may be molecular structure of the non-isomeric counterpart. Earlier reports show that in some polymers for example polyethylene oxide (PEO) and PEG with almost common O–C–C–O bond sequence acts as an effective electron donor and hence the direction of the dipole shall be along the backbone of the polymer[53]. Chemically, the dissimilarity in bond sequences which in our case consists of -C=N- may contribute to the electrical transport mechanism. However, we propose that the reasonable relaxation times calculated, could also be a function of the number of hydrogen bonds in amine (-NH$_2$-) functional group of polyaniline which must be excited to bring about orientation of dipoles in the presence of electric field.

Figure 5 clearly depicts the variation of $\Delta G^{\#}$ with temperature. From thermodynamics viewpoint, the negative nature of these values suggests that the reaction process is spontaneous and favours polyaniline formation. The values which are $\sim$ 2.3 times greater than the enthalpy change are quite comparable with results of Bhaumik et al.[54] and El-Naggar et al.[55]. All the estimated values of entropy $\Delta S^{\#}$ and that of enthalpy $\Delta H^{\#}$ were negative showing the degree of disorderliness of the proceeding reaction as delineated in Fig. 4 and exothermic nature of the polyaniline formation, respectively. From the plot, it was observed that there is an irregular order of the constituent molecules according to kinetic theory. In view of this, Whiffen and Thompson[32] and Hennelly
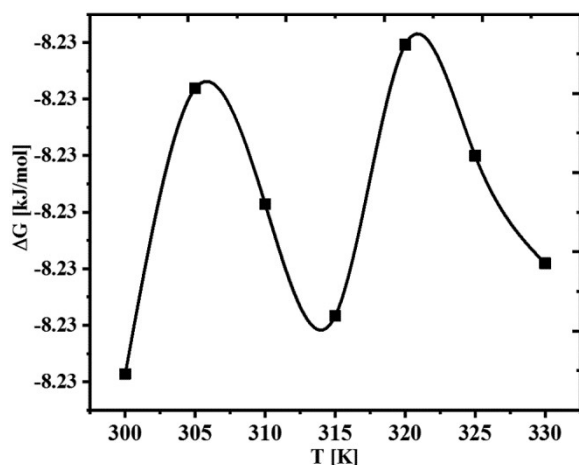
et al.[56] have emphasized on the importance of the negative sign of $\Delta S^{\#}$ as a means of making deductions from packing of molecules when compared with corresponding values of other systems. However, these authors further suggest that in the absence of sufficient information regarding the temperature dependence of these values, it may not present special significance other than indicating molecular configurations involved in dipole orientation possess activated state of greater local molecular order[33]. In any case, this is expected since entropy, a state function, depends on internal energy of the system which in sum is a function of temperature.

Figure 6 shows the SEM image ($\times$20k) which has a compact surface morphology in which randomly sized fibrous and elongated nanostructures are evenly distributed over the surface. The growth mechanism is believed to have taken off with rodlike structures which intertwine during polymerization. Before the growth process completes, the whole arrangement become meshy and fibrous. Therefore, the presence of free anilinium ions favours the microstructure in an additive manner via diffusion[57]. The formation of polyaniline was further confirmed by FTIR spectroscopy. The FTIR whose spectrum is shown in Fig. 7, have clearly visible absorption peaks. Generally, polyaniline possesses several distinct bands approximately at 3420, 1560, 1450, 1300, 1120 and 850 cm^{-1} which are identified specifically for the organic contents of polyaniline[58-60]. Functional group, triple and double bonds as well as fingerprint regions are characterized by 4000 – 2700, 1900 – 1500 and 1500 – 500 cm^{-1} ranges of wavenumber, respectively. Hence, the absorption of peaks at 3419 cm^{-1} and

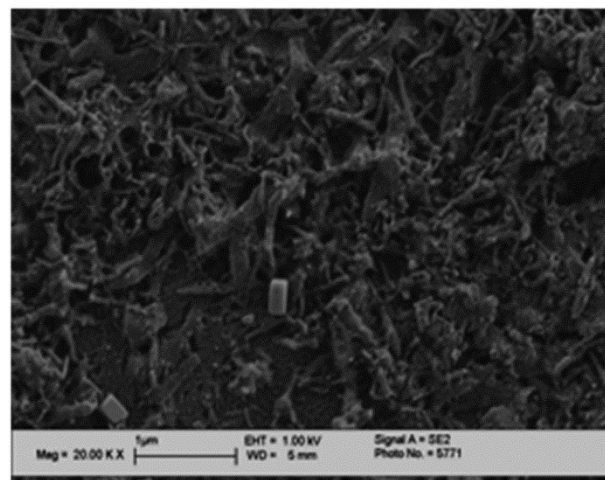Fig. 5 — Variation of Gibbs free energy $\Delta G^{\#}$ with temperature.

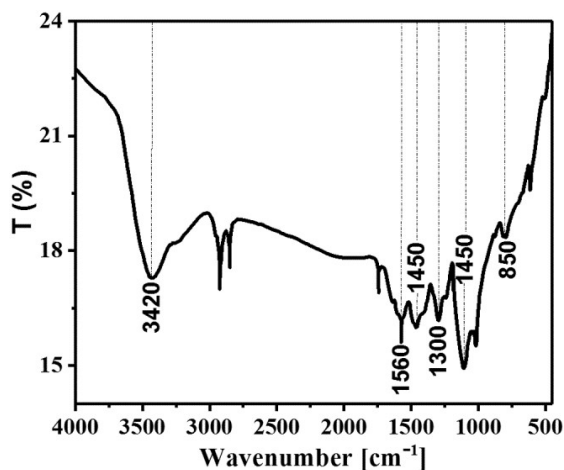Fig. 6 — Scanning electron microscopy of polyaniline film at ambient temperature.

Fig. 7 — Fourier transform-infrared spectroscopy of polyaniline film.

2923 cm^{-1} were due to stretching modes of the N―H and ―NH$_2^+$ bands of the aromatic ring in polyaniline. The peaks at 1594 cm^{-1} and 1461 cm^{-1} are attributed to the C=N stretching of quinonoid rings and also C=C stretching of benzenoid rings, respectively. The peaks at ~ 1290 cm^{-1} and 1147 cm^{-1} are characteristics of C―N=C bond stretching mode for benzenoid ring[61] while the peaks at ~ 1134 cm^{-1} and 820 cm^{-1} are specifically for out-of-plane bending vibration of C―H in benzene rings arising from the protonation process which affirms the successful formation of polyaniline during polymerization[58,62].

4 Conclusions

The kinetics, relaxation mechanism and activation parameters of polyaniline electrolyte in form of thin films have been studied via dielectric relaxation technique. Microscopically, the mechanism of conductivity shows an obvious temperature dependence which is linear and also an evidence of quantum tunnelling of charge carriers by reason of variable range hopping in localized states. Estimated thermodynamic parameters and activation energy show that the formation process is entirely diffusion controlled. The morphology has a compact surface with randomly sized fibrous and elongated nanostructures which are evenly distributed over the surface. The vibrational modes from FTIR spectroscopy which are acoustic confirmed the existence and formation of polyaniline structure.

References

1   Heeger A J, *Rev Mod Phys*, 73 (2011) 681.
2   DeGirolamo J, Reiss P, Zagorska M, De Bettignies R, Bailly S, Mevellec J Y, Lefrant S, Travers J P & Pron A, *Phys Chem Chem Phys*, 10 (2008) 4027.
3   Aldakov D, Jiu T, Zagorska M, de Bettignies R, Jouneau P H, Pron A & Chandezon F, *Phys Chem Chem Phys*, 12 (2010) 7497.
4   Zhu J, Wei S, Zhang L, Mao Y, Ryu J, Mavinakuli P, Karki A B, Young D P & Guo Z, *J Phys Chem C*, 114 (2010) 16335.
5   Ding K, Jia H, Wei S & Guo Z, *Ind Eng Chem Res*, 50 (2011) 7077.
6   Wei H, Yan X, Li Y, Wu S, Wang Y A, Wei S & Guo Z, *J Phys Chem C*, 116 (2012) 4500.
7   Wei H, Yan X, Li Y, Gu H, Wu S, Ding K, Wei S & Guo Z, *J Phys Chem C*, 116 (2012) 16286.
8   Li Y, Patil R, Wei S & Guo Z, *J Phys Chem C*, 115 (2011) 22863.
9   Wang C C, Song J F, Bao H M, Shen Q D & Yang C Z, *Adv Funct Mater*, 18 (2008) 1299.
10   Zhu J, Wei S, Zhang L, Mao Y, Ryu J, Haldolaarachchige N, Young D P & Guo Z, *J Mater Chem*, 21 (2011) 3952.
11   Huang J J & Kaner B R, *J Am Chem Soc*, 126 (2004) 851.
12   Catedral M D, Tapia A K G, Sarmago R V, Tamayo J P & del-Rosario E J, *J Sci Diliman*, 16 (2004) 41.
13   Hosseini S H, Dabiri M & Ashrafi M, *Polym Int*, 55 (2006) 1081.
14   Sharma H, *Conducting polymers: Polyaniline, its state of the art and applications*, Thesis, School of Physics and Materials Science, 2006.
15   Hosseini S H, Simiari J & Farhadpour B, *Iran Polymer J,* 18 (2009) 3.
16   Reddy K R, Sina B C, Ryua K S, Noh J & Lee Y, *J Synthetic Metals*, 159 (2009) 1934.
17   Vivekanandan J, Ponnusamy V, Mahudeswaran A & Vijayanand P S, *Arch Appl Sci Res,* 3 (2011) 147.
18   Zareh E H, Moghadam P N, Azariyan E & Sharifian I, *Iran Polymer J,* 20 (2011) 319.
19   Barros S B A, Leite C M S, de Brito A C F, Dos Santos Júnior J R, Zucolotto V & Eiras C, *Int J Anal Chem*, 116 (2012) 1.
20   Zotti G, Cattarin S & Comisso N, *J Electroana Chem Interfacial Electrochem*, 239 (1988) 387.
21   Liu X X, Zhang L, Li Y B, Bian L J & Su Z, *J Mater Sci*, 40 (2005) 4511.
22   Gu H, Tadakamalla S, Huang Y, Colorado H A, Luo Z, Haldolaarachchige N, Young D P, Wei S & Guo Z, *ACS Appl Mater Interfaces*, 4 (2012) 5613.
23   Zhu J, Gu H, Luo Z, Haldolaarachige N, Young D P, Wei S & Guo Z, *Langmuir*, 28 (2012) 10246.
24   Osaka T, *J Electrochem Soc*, 137 (1990) 2139.
25   Bhadra S, Khastgir D, Singha N K & Lee J H, *Prog Polymer Sci,* 34 (2009) 783.
26   Gospodinova N & Terlemezyan L, *Prog Polymer Sci*, 23 (1998) 1443.
27   Kalogeras I M, *Progress in polymer nanocomposite research*, (Eds. Thomas S & Zaikov G), Nova Science, Chap. 10, (2008).
28   Kremer F, Hartmann L Serghei, A, Pouret P & Leger L, *Eur Phys J*, 12 (2003) 139.
29   Hartmann L, Gorbatschow W, Hauwede J & Kremer F, *Eur Phys J*, 8 (2002) 145.
30   Nielsen O F, *Annu Rep Prog Chem Sect C*, 90 (1993) 3.
31   Buchner R & Barthel J, *Annu Rep Prog Chem Sect C*, 91 (1994) 71.

32   Whiffen D H & Thompson H W, *Trans Faraday Soc*, 41(1945) 180.
33   Hosamani M T, Ayachit N H & Deshpande D K, *J Therm Anal Calorim*, 107 (2012) 1301.
34   Coffey W T, *J Mol Liq*, 114 (2004) 5.
35   Kollengodu-Subramanian S & McKenna G B, *J Therm Anal Calorim*, 102 (2010) 477.
36   Me´sza´ros P & Funk D B, *J Therm Anal Calorim*, 82 (2005) 253.
37   Mano J, Lanceros-Me´ndez S, Nunes A & Dionı´sio M, *J Therm Anal Calorim*, 65 (2001) 37.
38   Sannaningannavar F M, Navati B S & Ayachit N H, *Polym Bull*, 73 (2016) 1689.
39   Higasi K, *Bull Chem Soc Jpn*, 39 (1966) 2157.
40   Higasi K, Koga Y & Nakamura M K, *Bull Chem Soc Jpn*, 44 (1971) 988.
41   Buchner R, Barthel J & Stauber J, *Chem Phys Lett*, 306 (1999) 57.
42   Patil V B, Pawar S G, Patil S L & Sood A K, *Orient J Chem*, 25 (2009) 945.
43   Xing S, Zhao C, Jing S & Wang Z, *Polymer*, 47 (2006) 2305.
44   Campos M & Bello J B, *J Phys D: Appl Phys*, 30 (1997) 1531.
45   Amaechi C I, Asogwa P U, Ekwealor A B C, Osuji R U, Maaza M & Ezema F I, *Appl Phys A*, 117 (2014) 1589.
46   Singh R, Arora V, Tandon R P, Mansingh A & Chandra S, *Synthetic Metals*, 104 (1999) 137.
47   Wang Z H, Scherr E M, MacDiarmid A G & Epstein A J, *Phys Rev B*, 45 (1992) 4190.
48   Spitzer W G & Fan H V, *Phys Rev*, 166 (1957) 882.
49   Zhu J, Gu H, Luo Z, Haldolaarachige N, Young D P, Wei S & Guo Z, *Langmuir*, 28 (2012) 10246.
50   Hedvig P, *Dielectric spectroscopy of polymers*, (Adam Hilger: Bristol), 1977.
51   Williams G, Landel R F & Ferry J D, *J Am Chem Soc*, 77 (1955) 3701.
52   Sannaningannavar F M, Navati B S & Ayachit N H, *J Appl Polym Sci*, 126 (2012) 375.
53   Sengwa R J, Kaur K & Choudhary R, *Polym Int*, 49 (2000) 599.
54   Bhaumik M, McCrindle R I, Maity A, Agarwal S & Gupta V K, *J Colloid Interface Sci*, 466 (2016) 442.
55   El-Naggar I M, Zakaria E S, Ali I M, Khalil M & El-Shahat M F, *Arab J Chem*, 5 (2012) 109.
56   Hennelly E J, Heston W M & Smyth C P, *J Am Chem Soc*, 70 (1948) 4102.
57   Li X, Li X, Dai N & Wang G, *Appl Surf Sci*, 255 (2009) 8276.
58   Li C, Wang J, Wen Y, Ning Y, Wen Y, Yuan X, Li M & Yang D, *ECS Electrochem Lett,* 2 (2013) H1.
59   Sariciftci N S, Kuzmany H, Neugebauer H & Neckel A, *J Chem Phys*, 92 (1990) 4530.
60   Trchova M, Sedenkova I & Stejskal J, *Synth Met*, 154 (2005) 1.
61   Kavitha B, Prabakar K, Kumar K S, Srinivasu D, Srinivas C, Aswal V K, Siriguri V & Narsimlu N, *IOSR J Appl Chem*, 2(2012) 16.
62   He Y, *Appl Surf Sci*, 249 (2005) 1.